3

Human Body Analysis

3.1 Introduction

The response of vehicle occupants to road inputs is an important factor in the design of any vehicle. A suspension ought to provide the greatest possible comfort.

On the other hand, on poor roads and in off-road operation, protection of the occupants from actual damage is most important. Tractor drivers in particular are at risk of lower-back injuries and possibly damage to viscera (liver, heart and brain).

In order to assess the merits of a suspension it is accordingly necessary to model the seat characteristics, particular those of the cushion. A model for the occupant(s) is also highly desirable, as will be described below.

The efficiency of isolation of 67 conventional seats and 33 suspension seats has been reported (Paddan and Griffin, 2002). The measure used was seat effective amplitude transmissibility (SEAT), which is the frequency-weighted root mean square acceleration experienced with the seat compared to that experienced with a rigid seat.

For 25 car seats the SEAT value varied between 57% and 122% with a median value of 78%. For the 16 trucks tested the SEAT range varied between 44% and 115%, with a mean of 87%. For seven tractors the SEAT value varied between 57% and 118%.

These results indicate the importance of good seat design. A key parameter is the characteristics of the foam material used for the seat.

Yu and Khameneh (1999) measured the transmissibility of three different types of foam formulations: two rather similar toluene diisocyanate (TDI) formulations, and one methylene diphenyl diisocyanate (MDI).

Using a shaped 50 kg load, displacement transmissibility for each foam was recorded over the range 2.5–6 Hz for inputs of 5 mm and 20 mm. At low-amplitude inputs (5 mm) the natural frequency was around 4 Hz. For all three foams, the natural frequency for 20 mm inputs was found to be about 0.5 Hz lower than that for 5 mm. The peak transmissibility was also reduced.

It is clear that the foams have a softening spring characteristic with damping ratio increasing with amplitude.

3.2 Human Body Response

Tests of 12 seated humans to vertical random acceleration in the range 0.2–20 Hz (Mansfield and Griffin, 2000) indicated that the human body also demonstrates a softening spring characteristic. The apparent mass resonance frequency fell from 5.4 Hz to 4.2 Hz as the magnitude of vibration increased from 0.25 m/s to 2.5 m/s. From these tests an equivalent mechanical system was developed (Wei and Griffin, 1998a and 1998b). While Wei and Griffin were careful to point out that no specific identification with parts of the body can be made, it appears plausible that this response is that of internal organs (viscera) within the skeleton. Excessive stretching of the intestinal attachment tissue (the mesentery) could lead to rupture and internal bleeding. Similarly the liver could be damaged, which implies serious implications for that vital organ. The visceral mass includes the brain, which *sloshes* within the skull. The issue here is that of pressure waves. Rebound of the brain causes reduced pressure which is thought to be the cause of concussion.

The resonant frequencies reported by Mansfield and Griffin for the human body are little greater than those found by Yu and Khameneh for mass foam cushions. The possibility of resonant interaction between cushion and occupant is quite possible. This may explain why some seats are significantly less comfortable than others.

Torsional chirp (swept sine) excitation of the wrist of subjects with forearm supported (Lakie *et al.*, 1984) indicated that the wrist resonant frequency fell markedly as the magnitude of the oscillatory input was increased. Here is evidence of the stiffness of tendons decreasing drastically with increasing force and hence displacement.

In view of the reported experimental work, it is plausible to adopt a spring force of the form $K(x-\varepsilon x^3)$, where K is the linear stiffness and $\varepsilon > 0$ for both foam and human body in the low-frequency range.

Hysteric damping is assumed and can be modelled via a complex stiffness $K(1+\mathrm{i}\beta)$, where β is the loss factor. This formulation guarantees non-linear damping which increases with amplitude, as will be shown below. The same form of damping in the human viscera is assumed as for foam.

3.3 Hysteretic Damping

For sinusoidal response (and the hysteretic model is really only valid for that condition) adopting the complex response:

$$x = A\mathrm{e}^{\mathrm{i}\omega t}, \tag{3.1}$$

$$\dot{x} = \mathrm{i}\,\omega\, x\,, \tag{3.2}$$

$$\dot{x}^3 = -\mathrm{i}\,\omega^3\, x^3, \tag{3.3}$$

The damping term is hence obtained as:

$$K\ \beta\left(\frac{\dot{x}}{\omega} + \varepsilon\left(\frac{\dot{x}}{\omega}\right)^3\right), \tag{3.4}$$

The non-linear term produces increased damping when $\varepsilon > 0$.
An effective damping ratio can be obtained as:

$$\zeta_{\text{eff}} = \frac{\omega_n\,\beta\left[1 + \varepsilon\left(\frac{\dot{x}}{\omega}\right)^2\right]}{2\,\omega}, \tag{3.5}$$

ω_n being the natural frequency of the linear system.
Assuming now that $x = C\,\sin(\omega t + \varphi)$, a mean damping of the form

$$\zeta_{\text{eff}} = \frac{\omega_n\,\beta\,(1 + 0.5\varepsilon\,C^2)}{2\,\omega} \tag{3.6}$$

can be obtained.

The frequency response of the system can be obtained and is useful in indicating the general behaviour of the system.

3.3.1 The Duffing Equation

A system governed by an equation of Duffing type (Hagerdon, 1998)

$$M\,\ddot{x} + B\,\dot{x} + K\left(x - \varepsilon\,x^3\right) = F\cos(\omega t + \varphi) \tag{3.7}$$

can exhibit jumps in amplitude if the damping is sufficiently low or the forcing F sufficiently large. Such jumps are undesirable, particularly so in the case of the visceral organs, where injury could result.

The type of behaviour is indicated in Figure 3.2 where the amplitude X of the response:

$$x = X\cos(\omega t) + \text{higher - order terms} \tag{3.8}$$

is plotted as a function of $p = \dfrac{\omega}{\omega_n}$, where $\omega_n = \left(\dfrac{K}{M}\right)^{0.5}$ is the natural frequency of the linear system.

For small F the response is virtually that of the linear system, but for larger values of F the response curves exhibit a buckled shape. For the top curve in Figure 3.1, as p is decreased slowly from a large value, when the point A is reached the response jumps to B. The critical condition is the vertical tangent. The solution at A is no longer real, while the formerly unreal solution at B becomes real.

As p is increased slowly again, when the point C is reached the response jumps to D (for a system in which the spring hardens with amplitude, the curves lean to the right).

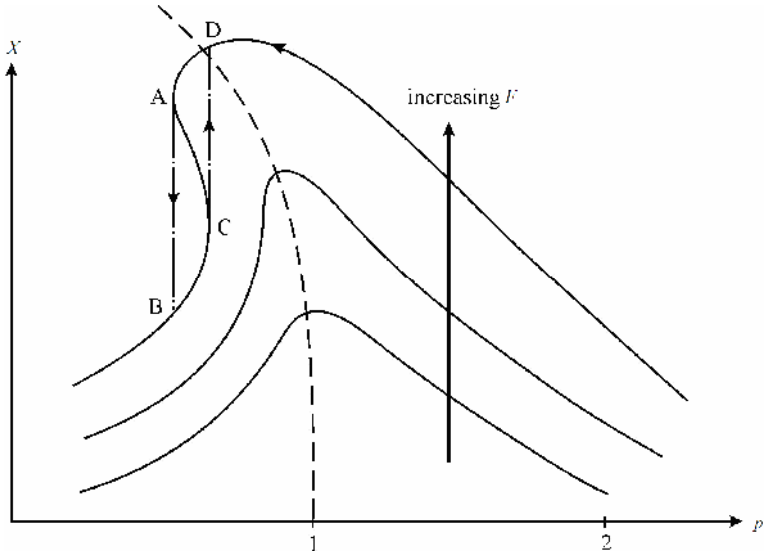

Fig. 3.1. Frequency response, softening spring; $p = \omega/\omega_n$

3.3.2 Suppression of Jumps

The loss factor β to prevent jumps can be obtained from the condition that no vertical tangent exists in the frequency response plot.

The equation of motion for a single-degree-of-freedom system has the form:

$$M\ddot{x} + K\beta\left(\frac{\dot{x}}{\omega} + \varepsilon\left(\frac{\dot{x}}{\omega}\right)^3\right) + K(x - \varepsilon x^3) = F_1\sin(\omega t) + F_2\cos(\omega t). \qquad (3.9)$$

It is convenient to non-dimensionalise the equation of motion by setting $\omega_n t = \tau$. The equation governing motion becomes

$$\ddot{x}+\beta\left(\frac{\dot{x}}{p}+\varepsilon\left(\frac{\dot{x}}{p}\right)^3\right)+\left(x-\varepsilon x^3\right)=\left(f_1\sin\left(p\tau\right)+f_2\cos\left(p\tau\right)\right), \tag{3.10}$$

where $f_j=F_j/M$, $p=\omega/\omega_n$ and differentiation is now with respect to τ.

Assuming a solution $x=C\sin\left(p\tau\right)$:

$$\left(1-p^2\right)C-\varepsilon C^3=f_1, \tag{3.11}$$

$$\beta C+\beta e C^3=f_2, \tag{3.12}$$

where

$$e=0.75\varepsilon. \tag{3.13}$$

Then

$$\left[\left(1-p^2\right)C-e\,C^3\right]^2+\left(\beta C+\beta e C^3\right)^2=f_1^2+f_2^2=f^2, \tag{3.14}$$

where f is a chosen input.

Jumps occur when $\frac{\partial C}{\partial p}$ is infinite, or more usefully, when $\frac{\partial p}{\partial C}=0$.

Differentiating (3.14) with respect to C, with the condition $\frac{\partial p}{\partial C}=0$

$$2\left[\left(1-p^2\right)C-eC^3\right]\left(1-p^2-3eC^2\right)+2\left(\beta C+\beta eC^3\right)\left(\beta+3\beta eC^2\right)=0. \tag{3.15}$$

Dividing by $2C$ and arranging as an equation in p

$$p^4-2p^2\left(1-2eC^2\right)+\left(1-3eC^2\right)\left(1-eC^2\right)+\beta^2\left(1+eC^2\right)\left(1+3eC^2\right)=0. \tag{3.16}$$

Jumps are impossible if this equation has no real roots for p^2, *i.e.*, if

$$\left(1-2\,e\,C^2\right)^2<\left(1-3\,e\,C^2\right)\left(1-e\,C^2\right)+\beta^2\left(1+eC^2\right)\left(1+3\,e\,C^2\right) \tag{3.17}$$

or

$$\beta^2>\frac{\left(1-2eC^2\right)^2-\left(1-3\,e\,C^2\right)\left(1-e\,C^2\right)}{\left(1+e\,C^2\right)\left(1+3\,e\,C^2\right)}, \tag{3.18}$$

i.e.,

$$\beta^2 > \frac{e^2\ C^4}{\left(1+e\ C^2\right)\left(1+3\ e\ C^2\right)}. \tag{3.19}$$

The value of β to suppress jumps is a function of eC^2. This is a measure of the magnitude of the nonlinear component of the spring force; see Equation 3.9. When $e\ C^2 << 1$, to prevent jumps it is necessary that

$$\beta > e\,C^2, \tag{3.20}$$

where $e = 0.75\ \varepsilon$.

For $e\ C^2 >> 1$, the required value of β to prevent all jumps is 0.58, greater than one would expect for human tissue. However, this is an extreme case.

Studies of the human visceral model with β around 0.3 (the level indicated by experimental work on cushions) suggest that jumps would occur for sinusoidal oscillations of the viscera in excess of 3 mm in magnitude. On the other hand, the value of β to prevent jumps of a foam cushion is less than 0.1.

3.4 Low-frequency Seated Human Model

Various detailed models of the human body exist. However, cushion and visceral natural frequencies are below 6 Hz. Moreover because the amplitude of road profile fluctuations falls with decreasing wavelength, road inputs experienced by vehicle occupants are predominantly at low frequency. For realistic vehicle speeds higher frequency inputs are not important until wheel-hop is experienced at around 12 Hz for cars and nearer 10 Hz for freight vehicles. When traversing rough ground, drivers instinctively slow, reducing the frequency of input. Hence a simple human model suitable for low-frequency inputs is adopted here.

The model adopted for the human body is one of those developed by Wei and Griffin (Wei and Griffin, 1998a). This is shown in the upper part of Figure 3.3. The non-linear spring K_v models stiffness effects with hysteretic effects providing damping.

The motion of the visceral mass M_v is denoted by x, and that of the remainder M_c of the body by y. This second mass could be that of the skeleton. The authors also produced a two-degree-of-freedom model in order to model response at frequencies greater than about 8 Hz. Vehicle simulations using this model indicated no significantly different response for realistic road inputs and vehicle speeds. Hence the single-degree-of-freedom model is adopted here.

The seat is modelled as a mass M_s and a (non-linear) spring K_s. As indicated above the damping terms are deduced from a hysteric model.

A seat control force F_c is considered. This would be provided by an actuator fixed to the vehicle floor beneath the seat.

The sprung mass M_s on a spring and damper suspension is modelled since it acts as a low-pass filter of road inputs. In the frequency range of interest, the unsprung mass is neglected, as is common with truck models.

The experimental work using vertical inputs indicates a natural frequency of the human body in the range 4.2–5.4 Hz, depending on the amplitude of input (Mansfield and Griffin, 2000). This is not far from the resonant frequencies reported for a loaded foam cushion (Yu and Khameneh, 1999).

3.4.1 Multi-frequency Input

Vehicle-occupant model for low-frequency vibration is depicted in Figure 3.2.

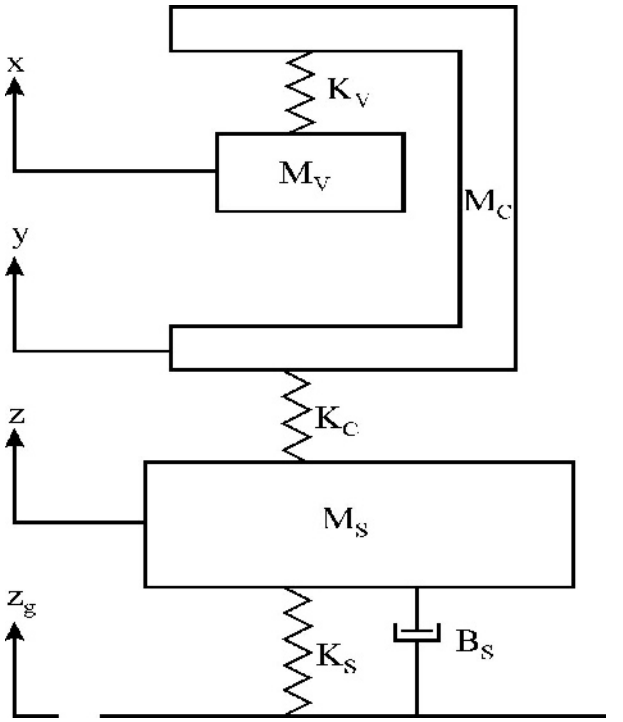

Fig. 3.2. Vehicle and occupant model (copyright Elsevier (1998), reproduced with minor modifications and with the addition of the bottom part of the figure from Wei and Griffin, The prediction of seat transmissibility from measures of seat impedance, J Sound Vib,Vol. 214, N 1, used by permission)

Ground input is indicated by z_g. The unsprung mass is not modelled as at the low frequencies considered (below 6 Hz) it follows the road.

M_s represents the sprung mass of the vehicle, restrained by a linear spring and viscous damper, as is commonly modelled.

The cushion is modelled as a complex spring K_c with loss factor β_c; M_c and M_v represent the two masses of the Wei and Griffin 1DOF model (Wei and Griffin, 1998b), with K_v a non-linear spring with loss factor β_v.

The equations of motion for an input z_g of frequency ω are:

$$\ddot{x} = \omega_v^2 \, u \left(1 - \varepsilon_v \, u^2\right) + \omega_v^2 \, \beta_v \, \dot{u} \frac{\left(1 + \varepsilon_v \frac{\dot{u}^2}{\omega^2}\right)}{\omega}, \tag{3.21}$$

$$\ddot{y} = -R \, \ddot{x} + (R+1)\omega_c^2 \, w \left(1 - \varepsilon_c \, w^2\right) + (R+1) \, \omega_c^2 \, \beta_c \, \dot{w} \frac{\left(1 + \varepsilon_c \frac{\dot{w}^2}{\omega^2}\right)}{\omega} + \frac{F_c}{M_c}, \tag{3.22}$$

$$\ddot{z} = \omega_s^2 \, \left(z_g - z\right) + 2 \, \zeta \, \omega_s \left(\dot{g} - \dot{z}\right) - \frac{F_c}{M_s} \tag{3.23}$$

where $u = y - x$, $w = z - y$ and $R = \frac{M_v}{M_c}$; ω_v is the natural frequency of the linear visceral system, ω_c is the natural frequency of the total mass $M_v + M_c$ on the linear cushion, ω_s is the natural frequency of the sprung mass on its suspension, z_g is the road surface displacement as experienced by the vehicle.

In the case of vehicles, the actual ground input is nearly always a multi-frequency input and the response similarly. The hysteretic damper analysis of Section 3.3 cannot now be employed.

The damping can be calculated by summing the contributions obtained from individual frequency inputs (Wettergren, 1997). However, this procedure requires the amplitude of vibration at each frequency to be known, calling for a continuous FFT of the response, which would not appear practical and would certainly add expense to the system. The somewhat less elegant solution of selecting a typical ω is the strategy adopted here.

The power spectral density for the road is defined over a range $[\Omega_1, \Omega_2]$ of the spatial frequency Ω (cycles/m); the frequency (Hz) experienced by a vehicle moving at speed V is $V\,\Omega$.

The excitation has the form $\sum a_j \sin\left(2\pi \Omega_j V t + \varphi_j\right)$, where Ω_j is a spatial frequency (cycles/m), V the vehicle speed and φ_j a random phase angle; $\dot{g}$ is the time derivative $\sum a_j \, 2 \, \pi \, \Omega_j V \cos\left(2\pi \Omega_j V t + \varphi_j\right)$ of the road surface displacement.

This model can be used to obtain the frequency response of the system, be it passive or controlled.

3.5 Semi-active Control

A semi-active device can only dissipate energy. Hence the damper can be on only when:

$$F_{\text{c, des}}\,\dot{w} < 0 \tag{3.24}$$

otherwise $F_{c,\,des}$ should be set to zero. This can be achieved in a dry friction control system by separating the plates. For a viscous damper or for a magnetorheological damper zero force is not possible and the best that can be achieved is to demand the minimal setting.

The response F_{c} of the actuator is assumed to be governed by a first-order system of the form:

$$T_{\text{const}}\,\dot{F}_{\text{c}} + F_{\text{c}} = F_{\text{c,des}}\,, \tag{3.25}$$

where T_{const} is the time for the error in the response to a step demand to fall to 36%.

The error caused by the non-zero time constant of the actuator can be reduced by a process of gain compensation. The demanded force is multiplied by a factor $\gamma > 1$, which is found to be effective when the integration time step is less than 20% of the actuator time constant. For zero error after one time constant, $\gamma = \left(1 - \mathrm{e}^{-1}\right)^{-1} = 1.58$.

As long as switching decisions are made several times a time constant, there should be no overshoot; the gain compensation procedure is found to reduce visceral accelerations by around 10% at vehicle speeds up to 20 m/s.

3.6 State Observer

To achieve comfort, it is necessary to reduce the acceleration $\ddot{x}$ of the viscera. This could be achieved if the relative internal displacement u and relative velocity $\dot{u}$ could be controlled. However, it is not possible in practice to measure these quantities.

It is therefore necessary to construct a state observer. The observer concept was first proposed by Luenberger (1964).

3.6.1 Luenberger State Observer

The most general case is the one in which no state variable are measured. This is termed the full-order observer.

Consider a system with state variables $\boldsymbol{x} = [x_1\,,\, x_2\,, \ldots,\, x_n]$ which generates an output $\boldsymbol{y} = \boldsymbol{C}\,\boldsymbol{x}$ which can be measured.

If the system dynamics are given by

$$\dot{\boldsymbol{x}} = \boldsymbol{A}\boldsymbol{x} + \boldsymbol{B}\boldsymbol{u}\ , \tag{3.26}$$

where $\boldsymbol{u}$ is a vector of control inputs, an estimate $\boldsymbol{z}$ of $\boldsymbol{x}$ is given by the equation

$$\dot{\boldsymbol{z}} = \boldsymbol{A}\boldsymbol{z} + \boldsymbol{B}\boldsymbol{u} + \boldsymbol{K}(\boldsymbol{y} - \boldsymbol{C}\boldsymbol{z}) \tag{3.27}$$

and $\boldsymbol{K}$ is the observer gain matrix, the error $\boldsymbol{e} = \boldsymbol{x} - \boldsymbol{z}$ is found to satisfy

$$\dot{\boldsymbol{e}} = (\boldsymbol{A} - \boldsymbol{K}\boldsymbol{C})\boldsymbol{e}\ . \tag{3.28}$$

The estimate $\boldsymbol{z}$ of $\boldsymbol{x}$ is governed by:

$$\dot{\boldsymbol{z}} = (\boldsymbol{A} - \boldsymbol{K}\boldsymbol{C})\boldsymbol{z} + \boldsymbol{B}\boldsymbol{u} + \boldsymbol{K}\boldsymbol{y}\ . \tag{3.29}$$

If the eigenvalues of the matrix $\boldsymbol{A} - \boldsymbol{K}\boldsymbol{C}$ are chosen suitably (by an appropriate choice of $\boldsymbol{K}$) the error $\boldsymbol{e} = \boldsymbol{x} - \boldsymbol{z}$ should decay rapidly.

The calculation of $\boldsymbol{K}$ involves, among other steps, the formation of a controllability matrix and an observability matrix, and is not simple. The reader is referred to Crossley and Porter (1979) or Burns (2001) for details.

In many cases, as in the application considered here, some of the variables (such as seat relative displacement and relative velocity) can be measured. However, what cannot be measured are the displacement and velocity of the viscera relative to the skeleton and the skeleton relative to the seat. In the case where only some of the state variables need to be estimated, the observer is known as a reduced-order state observer.

A similar mathematical path is required for the generation of $\boldsymbol{K}$ as in the full-order observer.

3.6.2 Simple State Observer

The method outlined here (Stammers and Sireteanu, 2004) requires no pre-processing, and is simple enough to be implemented in real time.

The relative acceleration $\ddot{u}$ can be expressed from (3.21) and (3.22) as

$$\begin{aligned}\ddot{u} = -K_{\mathrm{v}}\left(\frac{1}{M_{\mathrm{v}}} + \frac{1}{M_{\mathrm{c}}}\right)u\left(1 - e_{\mathrm{v}}\,u^2\right) - \frac{\beta_{\mathrm{v}}\,K_{\mathrm{v}}\left(\dfrac{1}{M_{\mathrm{v}}} + \dfrac{1}{M_{\mathrm{c}}}\right)\dot{u}\left(1 + \varepsilon_{\mathrm{v}}\dfrac{\dot{u}^2}{\omega^2}\right)}{\omega} \\ + \frac{K_{\mathrm{c}}\,w\left(1 - \varepsilon_{\mathrm{c}}\,w^2\right)}{M_{\mathrm{c}}} + K_{\mathrm{c}}\,\beta_{\mathrm{c}}\,\dot{w}\,\frac{\left(1 + \varepsilon_{\mathrm{c}}\dfrac{\dot{w}^2}{\omega^2}\right)}{\omega\,M_{\mathrm{c}}} + \frac{F_{\mathrm{c}}}{M_{\mathrm{c}}}.\end{aligned} \tag{3.30}$$

If F_{c} is chosen so that

$$K_c\, w\frac{\left(1-\varepsilon_c\, w^2\right)}{M_c}+\frac{K_c\,\beta_c\;\dot{w}\left(1+\varepsilon_c\,\dfrac{\dot{w}^2}{\omega^2}\right)}{\omega\; M_c}+\frac{F_c}{M_c}=0 \tag{3.31}$$

whenever control is possible, u is the response of a damped oscillator and will decay toward zero. The relative displacement w and relative velocity $\dot{w}$ of the seat with respect to the sprung mass can be obtained by the use of an LVDT or a pull-wire transducer.

Alternatively the accelerations of the seat and the vehicle floor could be recorded and the difference integrated and low-pass filtered to obtain the relative velocity and displacement, although this system might be more expensive than that needed for the displacement method.

If the system were active and the time constant of the device low enough, the relative displacement and velocity of the viscera could be driven to zero and no discomfort would be experienced.

For the semi-active device to be on it is necessary that power be dissipated, namely that

$$F_c\,\dot{w}<0\,. \tag{3.32}$$

Experience with a semi-active control for a random input shows that the damper can only be on about half of the time.

3.6.3 Ideal Control

The performance of the proposed observer can be assessed by a comparison with the ideal situation in which the relative displacement u and its derivative are known.

In this case reference to Equation (3.30) shows that F_c should be chosen to satisfy

$$\begin{aligned}&-K_v\left(\frac{1}{M_v}+\frac{1}{M_c}\right)u\,\left(1-\varepsilon_v\,u^2\right)-\frac{\beta_v\,K_v\left(\dfrac{1}{M_v}+\dfrac{1}{M_c}\right)\dot{u}\left(1+\varepsilon_v\,\dfrac{\dot{u}^2}{\omega^2}\right)}{\omega}+\\&+\frac{K_c\,w\left(1-\varepsilon_c\,w^2\right)}{M_c}+\frac{K_c\,\beta_c\,\dot{w}\left(1+\varepsilon_c\,\dfrac{\dot{w}^2}{\omega^2}\right)}{\omega\,M_c}+\frac{F_c}{M_c}=0.\end{aligned} \tag{3.33}$$

3.7 Results

The value of ε_c was estimated from the transmission ratios found experimentally by Yu and Khameneh (1999). Their work indicated that ε_c is approximately 400 m^{-2}. The results of Yu and Khameneh were also used to obtain values of f_c and β_c. Values of 4.35 Hz and 0.375 Hz, respectively, were deduced. The work of Mansfield and Griffin (2000) suggests ε_v is approximately 5000 m^{-2}.

Figure 3.3 shows the loss factor β required to prevent jumps in the cushion and viscera as a function of amplitude of response C.

The required value of β for the cushion is sufficiently low that even with oscillations of 20 mm amplitude, jumps will not in practice occur.

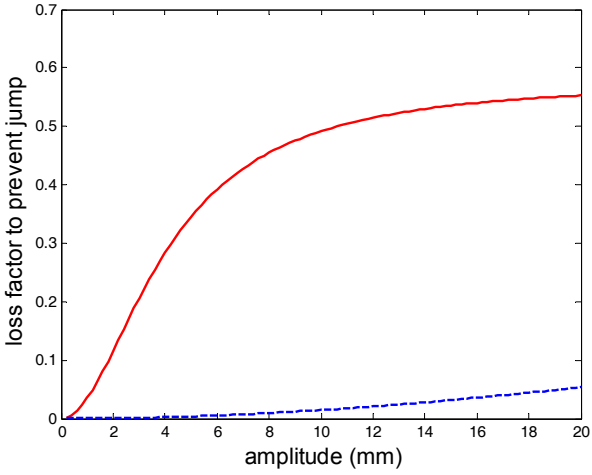

Fig. 3.3. Loss factor β to prevent jumps as a function of amplitude: viscera (solid line), cushion (dashed line)

The corresponding results for viscera indicate that, if visceral input oscillations are kept below 2 mm, a value of β_v of only 0.1 or greater is required. If on the other hand oscillations of up to 4 mm in amplitude occured, β_v would need to be greater than 0.3 (of similar magnitude to that estimated for cushion material) to prevent jumps. Jumps in the viscera would be physically damaging quite apart from the effect of the oscillation itself. The value of β_v likely to exist is not known but such predictions appear quite credible.

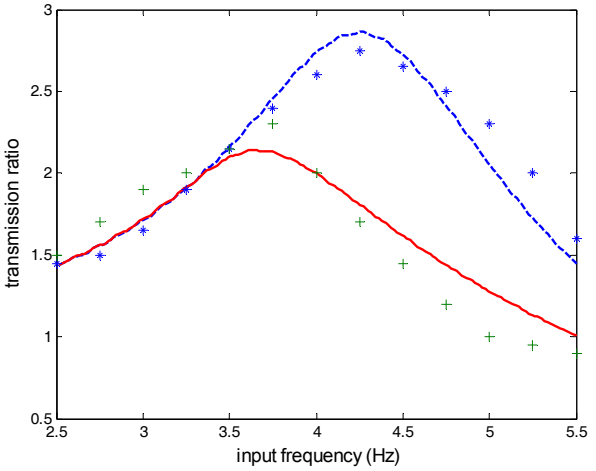

Fig. 3.4. Comparison of predicted (solid curves) and measured cushion transmissibility, * 5 mm input, + 20 mm input (measured data reproduced from Yu and Khameneh, Automotive seating foam: subjective dynamic comfort study. Reprinted with permission from SAE Paper # 1999-01-0588 © 1999 SAE International)

In Figure 3.4 the quoted transmissibility for cushion *C* (acc. out/acc. in) is compared with the predicted value for sinusoidal inputs of amplitude (a) 5 mm and (b) 20 mm; $\beta_c = 0.3$, $\varepsilon_c = 100$ N/m^3 and $f_n = 4.25$ Hz.

Agreement is quite good for the 5 mm inputs, and fair for the 20 mm inputs. Higher-order stiffness effects could be introduced if required.

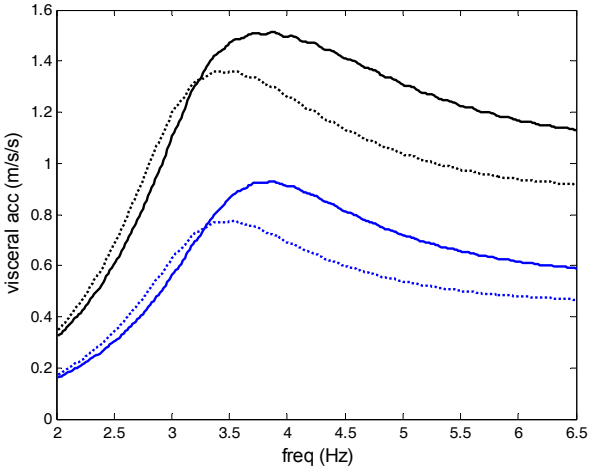

Fig. 3.5. $\varepsilon_v = 5000$ m^{-2}, $\varepsilon_c = 100$ m^{-2}, $\beta = 0.3$ for both viscera and cushion; viscera $f_v = 5$ Hz. Solid lines: $f_c = 4.75$ Hz, dashed lines: $f_c = 4$ Hz. Lower curves: 1 mm input, upper curves: 2 mm input

With 2 mm seat input (Figure 3.5), a cushion with f_c = 4.75 Hz has a peak visceral acceleration input (upper curves) which is 11% greater than that for f_c = 4 Hz. However, for 1 mm input (lower curves) the increase in peak acceleration is 20%.

Due to nonlinear damping, doubling the input increases the peak response by only 67%. The shift of peak response with increased magnitude of input is modest but detectable.

The effect of a simple observer is shown in Figures 3.6 as a frequency response plot and in Figure 3.7 for a random road input. The observer removes the resonance at around 3.5 Hz.

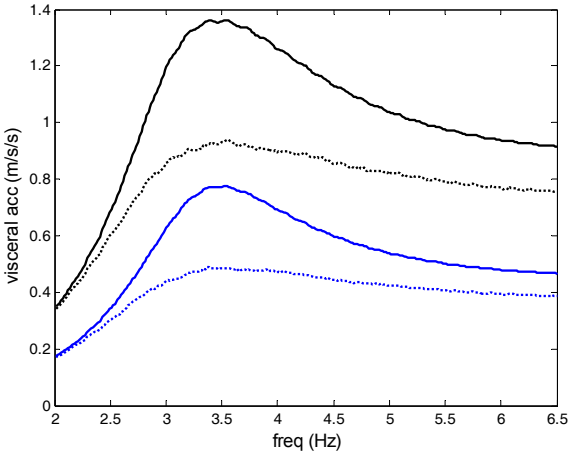

Fig. 3.6. ε_v = 5000 m^{-2}, ε_c = 100 m^{-2}, $\beta_c = \beta_v$= 0.4, f_c = 4 Hz, f_v = 5 Hz. Observer-based seat control (dotted) versus passive case (solid) for inputs of 1 mm (lower curves) and 2 mm (upper curves)

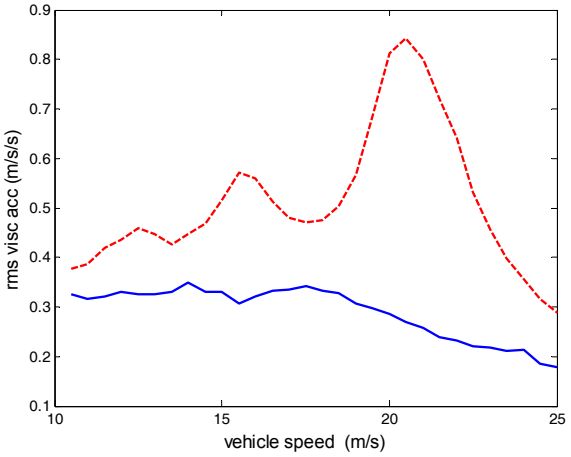

Fig. 3.7. Visceral response passive (dashed), simple observer (solid line); data as above

3.8 Seated Human with Head-and-Neck Complex

The seated human model has four subsystems: seat, cushion, driver body and the head-and-neck complex (HNC). The latter is represented as an inverted double pendulum.

The entire seated human model, together with the seat mass and under seat semi-active damper, is presented in Figure 3.8.

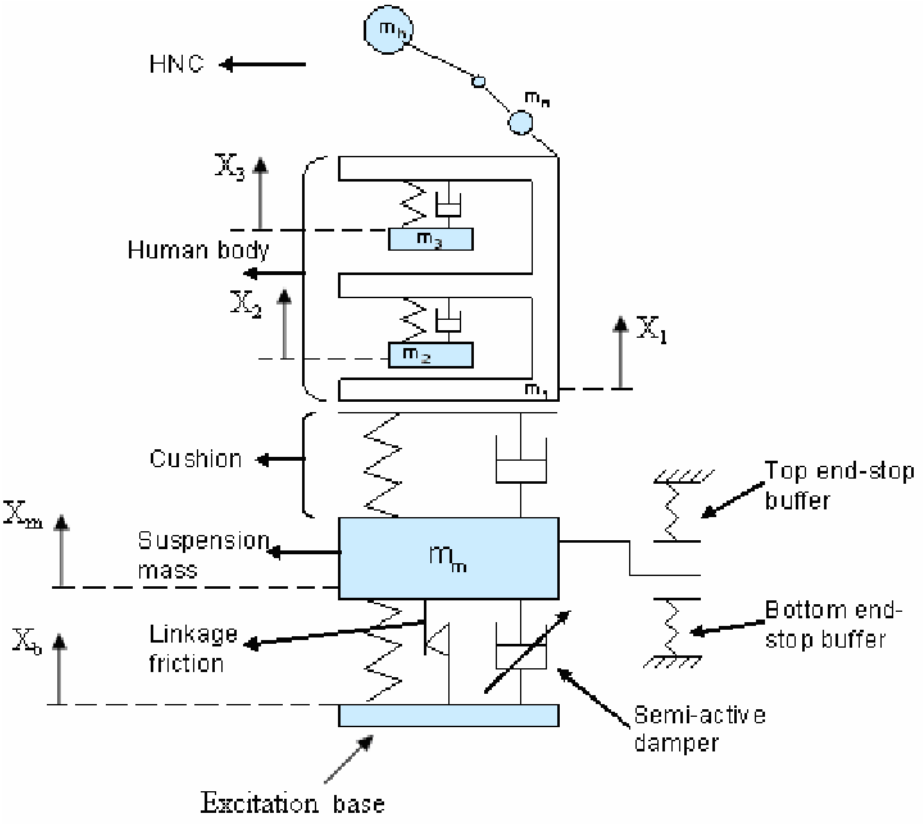

Fig. 3.8. Schematic diagram of the seated human model with HNC

The equations of motion for the body and seat are:

$$m_3 \ddot{x}_3 = C_3 \left(\dot{x}_1 - \dot{x}_3\right) + K_3 \left(x_1 - x_3\right) = f_3(t), \tag{3.34}$$

$$m_2 \ddot{x}_2 = C_2 \left(\dot{x}_1 - \dot{x}_2\right) + K_2 \left(x_1 - x_2\right) = f_2(t), \tag{3.35}$$

$$m_1 \ddot{x}_1 = C_c \left(\dot{x}_s - \dot{x}_1\right) + K_c \left(x_s - x_1\right) - f_2(t) - f_3(t), \tag{3.36}$$

$$m_m \ddot{x}_s = F_c(t) + K_s \left(z_0 - x_s\right) - C_c \left(\dot{x}_s - \dot{x}_1\right) - \left(x_s - x_1\right) + F_{bw}(t) + F_{buffer}(t). \tag{3.37}$$

$$\dot{F}_{bw} = \left(k - K_s\right)\dot{z} - \gamma \left|\dot{z}\right| F_{bw} - \beta \dot{z} \left|\dot{F}_{bw}\right|, \tag{3.38}$$

$$F_{buffer} = \begin{cases} k_1^t \left(z_o - x_s - d\right) + C_1 \dot{z} & \text{if } \left(z_o - x_s\right) > d \\ k_1^b \left(z_o - x_s + d\right) + k_3^b \left(z_o - x_s + d\right)^3 & \text{if } \left(z_o - x_{ss}\right) < -d \end{cases} \tag{3.39}$$

The non-linearity of the system is modelled by Equations 3.38 and 3.39 using the Bouc–Wen method to describe the linkage suspension friction and the end-stop buffers to protect the system from high-amplitude vibration, respectively.

3.8.1 Driver Seat (Including Cushions)

A typical truck seat is made of a frame that usually contains some sort of suspension, and foam pads covered with fabric or leather. Cushions are commonly used in the car industry to protect the human spine and body from vibration due to road irregularities. The material and the design of foam pads may differ, hence one cushion may protect the occupant, while another amplifies the input vibration.

Seat cushions generally have nonlinear characteristics (Yu and Khameneh, 1999). Nonlinear hysteretic damping analysis is used here to model such effects.

The model used is shown in Figure 3.9. End-stop buffers are used in order to protect the system from severe vibration with high amplitude. This system is modelled as nonlinear stiffness elements in terms of fifth-order polynomial functions. The coefficients of these polynomials were determined by applying a least-square curve fit to the measured buffer force–deflection characteristic (Gunston *et al.*, 2004).

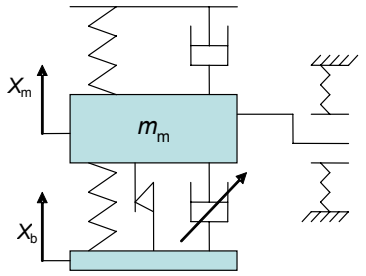

Fig. 3.9. Non-linear driver seat model

The input to the driver seat is the motion of the vehicle chassis which is combined heave and pitch. Only the vertical component is considered in the body response analysis.

3.8.2 Driver Body

The driver model (Figure 3.10) is based on experimental work of Wei and Griffin and consists of a light frame (m_1) and two suspended masses (m_2 and m_3) each with a linear spring and damper. The three masses do not represent actual human organs but are chosen so that the model reproduces the force response of vibrated subjects.

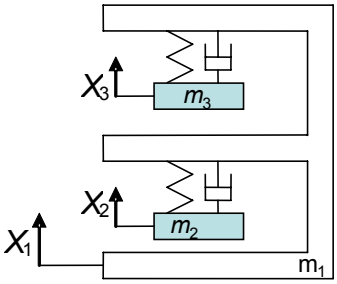

Fig. 3.10. Driver body model [copyright Elsevier (1998), reproduced with modifications from Wei and Griffin, The prediction of seat transmissibility from measures of seat impedance, J Sound Vib,Vol 214, N 1, pp 121–137, used by permission]

3.8.3 Head-and-Neck Complex (HNC)

A two-degree-of-freedom model (Figure 3.8) is used to describe the head-and-neck system (Fard *et al.*, 2003); a linearised model of the double inverted pendulum is used to emulate the motion of the head-and-neck complex. The first centre of rotation is assumed to be very close to the centre of the neck O_2, while the second centre of rotation is situated at O_1.

The determination of the viscoelastic parameters is a very difficult task that requires much experimental work and data with human volunteers. Based on published work of Fard *et al.* (2003) these parameters are summarised in Table 3.1. The head-and-neck complex is attached to the driver body in order to represent the human seated model including the driver body and the head-and-neck motion. For vehicle applications the driver body is assumed to vibrate in the vertical direction only, while the HNC is able to rotate in three dimensions in response to driver body vertical motion and the vertical, pitch and lateral motion of the vehicle chassis. The HNC system for 3D analysis is described using the Gibbs–Appel method.

Table 3.1. Head-and-neck complex parameters (copyright Elsevier, reproduced from Tsampardoukas G, Stammers CW and Guglielmino E, Hybrid balance control of a magnetorheological truck suspension, accepted for publication in J Sound Vib, used by permission)

Parameter	Value
L_{1p}	0.042 m
m_{1p}	1.07 kg
J_1	0.0012 kgm^2
L_{2p}	0.071 m
m_{2p}	4.31 kg
J_2	0.0216 kgm^2
K_{1p}	15.57 Nm/rad
C_{1p}	0.358 Nms/rad
K_{2p}	10.45 Nm/rad
C_{2p}	0.266 Nms/rad

3.8.4 Analysis of the Head-and-Neck System

The motion of the head-and-neck complex (HNC) due to vertical, pitch and roll motions of the vehicle chassis is presented using the Gibbs–Appel method (Blundell and Harty, 2004), an alternative method to Lagrange. With the Gibbs–Appel method the kinetic energy of the Lagrange method is replaced with the "energy" of acceleration. The potential energy of the system (Equation 3.46) is used just as with the Lagrange method. In complicated systems, Gibbs–Appel can be a simpler tool than Lagrange for the derivation of the equations of motion.

The Appel function A of the system (the acceleration "energy") in three dimensions is presented in Equation 3.47. Equations of motion are obtained via derivation of the total acceleration of each direction as presented by Equations 3.48–3.51.

The external accelerations (Figures 3.11 and 3.12) applied both to the head and neck due to the motion of the vehicle chassis are given by Equations 3.40–3.42, taking into account that the pitch and roll chassis accelerations can be analysed into two components, one vertical and one horizontal. The component in lateral direction is not illustrated in Figures 3.11 and 3.12.

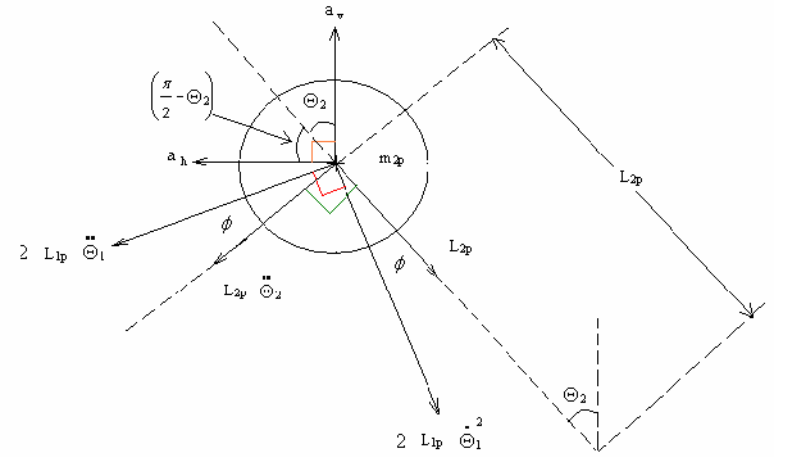

Fig. 3.11. Head accelerations [copyright IMechE (2008), reproduced from Tsampardoukas G, Stammers CW and Guglielmino E, Semi-active control of a passenger vehicle for improved ride and handling, accepted for publication in Proceedings of the Institution of Mechanical Engineers, Part D: Journal of Automobile Engineering, Publisher: Professional Engineering Publishing, ISSN 0954/4070, Vol 222, D3/2008, pp 325–352, used by permission]

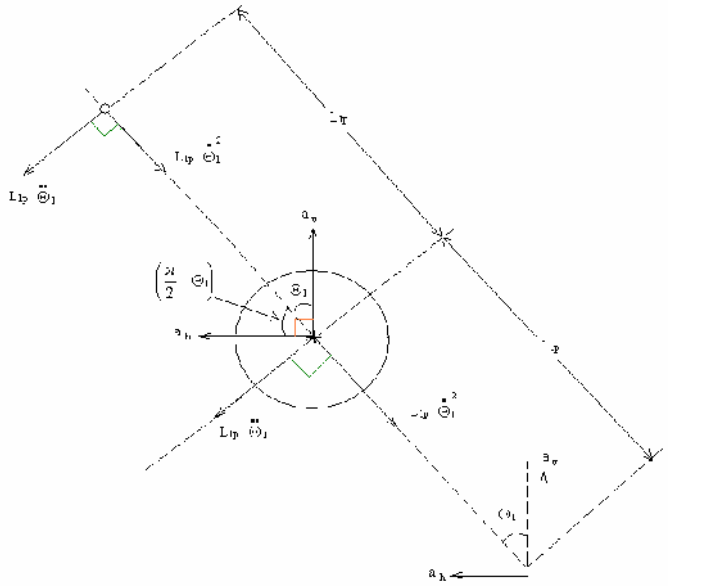

Fig. 3.12. Neck accelerations [copyright IMechE (2008), reproduced from Tsampardoukas G, Stammers CW and Guglielmino E, Semi-active control of a passenger vehicle for improved ride and handling, accepted for publication in Proceedings of the Institution of Mechanical Engineers, Part D: Journal of Automobile Engineering, Publisher: Professional Engineering Publishing, ISSN 0954/4070, Vol 222, D3/2008, pp 325–352, used by permission]

The accelerations a_v, a_h and a_z in the vertical, longitudinal and lateral directions, respectively are used to form A_x, A_y and A_z, the Appel function in terms of axes fixed in the head.

$$a_v = \ddot{X}_c + L_3 \ddot{\Theta}_C + \frac{L}{4} \ddot{\Phi}_C , \tag{3.40}$$

$$a_h = h_p \ddot{\Theta}_C , \tag{3.41}$$

$$a_z = h_p \ddot{\Phi}_C , \tag{3.42}$$

$$\begin{aligned} A_x = {} & \frac{1}{2} m_2 \left(a_v \sin(\Theta_2) - a_h \cos(\Theta_2) - 2 L_1 \ddot{\Theta}_1 \cos(\Phi) - L_2 \ddot{\Theta}_2 - 2 L_1 \dot{\Theta}_1^2 \sin(\Phi)\right)^2 \\ & + \frac{1}{2} m_1 \left(a_v \sin(\Theta_1) - a_h \cos(\Theta_2) - L_1 \ddot{\Theta}_1\right)^2, \end{aligned} \tag{3.43}$$

$$\begin{aligned} A_y = {} & \frac{1}{2} m_2 \begin{pmatrix} a_v \cos(\Theta_2) + a_h \sin(\Theta_2) + 2 L_1 \ddot{\Theta}_1 \sin(\Phi) - L_2 \dot{\Theta}_2^2 - 2 L_1 \dot{\Theta}_1^2 \cos(\Phi) \\ + a_v \cos(\Phi_{2roll}) + a_z \sin(\Phi_{2roll}) + 2 L_1 \ddot{\Phi}_{1roll} \sin(\Phi_{roll}) - L_2 \dot{\Phi}_{2roll}^2 \\ - 2 L_1 \dot{\Phi}_{1roll}^2 \cos(\Phi_{roll}) \end{pmatrix}^2 \\ & + \frac{1}{2} m_1 \begin{pmatrix} a_v \cos(\Theta_1) + a_h \sin(\Theta_1) - L_1 \dot{\Theta}_1^2 + a_v \cos(\Phi_{1roll}) + a_z \sin(\Phi_{1roll}) \\ - L_1 \dot{\Phi}_{1roll}^2 \end{pmatrix}^2, \end{aligned} \tag{3.44}$$

$$\begin{aligned} A_z = {} & \frac{1}{2} m_2 \begin{pmatrix} a_v \sin(\Phi_{2roll}) - a_z \cos(\Phi_{2roll}) - 2 L_1 \ddot{\Phi}_{1roll} \cos(\Phi_{roll}) - L_2 \ddot{\Phi}_{2roll} \\ - 2 L_1 \dot{\Phi}_{1roll}^2 \sin(\Phi_{roll}) \end{pmatrix}^2 \\ & + \frac{1}{2} m_1 \left(a_v \sin(\Phi_{1roll}) - L_1 \ddot{\Phi}_{1roll} - a_z \cos(\Phi_{1roll})\right)^2, \end{aligned} \tag{3.45}$$

$$
\begin{aligned}
PE = {} & m_1 L_1 g \cos(\Theta_1) + m_2 g \left(2 L_1 \cos(\Theta_1) + L_2 \cos(\Theta_2)\right) + \frac{1}{2} K_2 (\Theta_2 - \Theta_1)^2 \\
& + \frac{1}{2} C_2 \left(\dot{\Theta}_2 - \dot{\Theta}_1\right)^2 + \frac{1}{2} K_1 \Theta_1^2 + \frac{1}{2} C_1 \dot{\Theta}_1^2 + m_1 L_1 g \cos(\Phi_{1\text{roll}}) \\
& + m_2 g \left(2 L_1 \cos(\Phi_{1\text{roll}}) + L_2 \cos(\Phi_{2\text{roll}})\right) + \frac{1}{2} K_2 (\Phi_{2\text{roll}} - \Phi_{1\text{roll}})^2 \\
& + \frac{1}{2} C_2 \left(\dot{\Phi}_{2\text{roll}} - \dot{\Phi}_{1\text{roll}}\right)^2 + \frac{1}{2} K_1 \Phi_1^2 + \frac{1}{2} C_1 \dot{\Phi}_1^2,
\end{aligned}
\tag{3.46}
$$

$$
A = A_x + A_y + A_z \,, \tag{3.47}
$$

The equations of motion are:

$$
\frac{\partial A}{\partial \ddot{\Theta}_1} + \frac{\partial PE}{\partial \dot{\Theta}_1} + \frac{\partial PE}{\partial \Theta_1} = 0 \Leftrightarrow \frac{\partial A_x}{\partial \ddot{\Theta}_1} + \frac{\partial A_y}{\partial \ddot{\Theta}_1} + \frac{\partial A_z}{\partial \ddot{\Theta}_1} + \frac{\partial PE}{\partial \dot{\Theta}_1} + \frac{\partial PE}{\partial \Theta_1} = 0 \,, \tag{3.48}
$$

$$
\frac{\partial A}{\partial \ddot{\Theta}_2} + \frac{\partial PE}{\partial \dot{\Theta}_2} + \frac{\partial PE}{\partial \Theta_2} = 0 \Leftrightarrow \frac{\partial A_x}{\partial \ddot{\Theta}_2} + \frac{\partial A_y}{\partial \ddot{\Theta}_2} + \frac{\partial A_z}{\partial \ddot{\Theta}_2} + \frac{\partial PE}{\partial \dot{\Theta}_2} + \frac{\partial PE}{\partial \Theta_2} = 0 \,, \tag{3.49}
$$

$$
\frac{\partial A}{\partial \ddot{\Phi}_{1\text{roll}}} + \frac{\partial PE}{\partial \dot{\Phi}_{1\text{roll}}} + \frac{\partial PE}{\partial \Phi_{1\text{roll}}} = 0 \Leftrightarrow \frac{\partial A_x}{\partial \ddot{\Phi}_{1\text{roll}}} + \frac{\partial A_y}{\partial \ddot{\Phi}_{1\text{roll}}} + \frac{\partial A_z}{\partial \ddot{\Phi}_{1\text{roll}}} + \frac{\partial PE}{\partial \dot{\Phi}_{1\text{roll}}} + \frac{\partial PE}{\partial \Phi_{1\text{roll}}} = 0, \tag{3.50}
$$

$$
\frac{\partial A}{\partial \ddot{\Phi}_{2\text{roll}}} + \frac{\partial PE}{\partial \dot{\Phi}_{2\text{roll}}} + \frac{\partial PE}{\partial \Phi_{2\text{roll}}} = 0 \Leftrightarrow \frac{\partial A_x}{\partial \ddot{\Phi}_{2\text{roll}}} + \frac{\partial A_y}{\partial \ddot{\Phi}_{2\text{roll}}} + \frac{\partial A_z}{\partial \ddot{\Phi}_{2\text{roll}}} + \frac{\partial PE}{\partial \dot{\Phi}_{2\text{roll}}} + \frac{\partial PE}{\partial \Phi_{2\text{roll}}} = 0, \tag{3.51}
$$

The equations of motion for the head-and-neck complex in three dimensions are obtained. In matrix form:

$$
\boldsymbol{M}(\boldsymbol{q})\ddot{\boldsymbol{q}} + \boldsymbol{B}(\boldsymbol{q})\,\dot{\boldsymbol{q}}^2 + \boldsymbol{C}\,\dot{\boldsymbol{q}} + \boldsymbol{D}\,\boldsymbol{q} + \boldsymbol{E}(\boldsymbol{q})\sin(\boldsymbol{q}) = \boldsymbol{P}(\boldsymbol{q})\,\boldsymbol{U} \,, \tag{3.52}
$$

where

$$
\boldsymbol{q} = \begin{bmatrix} \Theta_1 \\ \Theta_2 \\ \phi_{1\text{roll}} \\ \phi_{2\text{roll}} \end{bmatrix}, \quad \boldsymbol{U} = \begin{bmatrix} U_{\text{V}} \\ U_{\text{H}} \\ U_{\text{Z}} \end{bmatrix}
$$

These equations can be then incorporated with those for the seat and body.

3.8.5 Head Accelerations During Avoidance Manoeuvre

The acceleration of the driver's head during an avoidance manoeuvre (modelled as a rapid lane change) are shown in Figure 3.13 as a function of vehicle speed. The performance of three different algorithms for the semi-active control (discussed subsequently in Chapters 4 and 7) of the suspension, namely skyhook, balance control cancelling (BCC) and balance control additive (BCA).

Skyhook was designed to achieve improved ride, and the benefit of skyhook control compared with the passive case is evident in all three directions — longitudinal, vertical and lateral. The BCC algorithm was designed to limit dynamic tyre loads and hence reduce road damage in the case of heavy vehicles. It is of no help to the driver in terms of comfort, but is very helpful in improving handling and thus achieving the intended rapid lane change. The BCA algorithm is employed to reduce vehicle roll. This is important for a laden freight vehicle which will have a higher centre of gravity, but is of secondary importance for a passenger vehicle. The switching between different algorithms depending on the driving conditions could be implemented automatically on the basis of some feedback indicators. This could be made in a variety of ways. A possible approach could be using a rapid steering input at high speeds to select the BCC algorithm (to achieve improved safety). Conversely at lower speeds, skyhook could be selected for driver comfort.

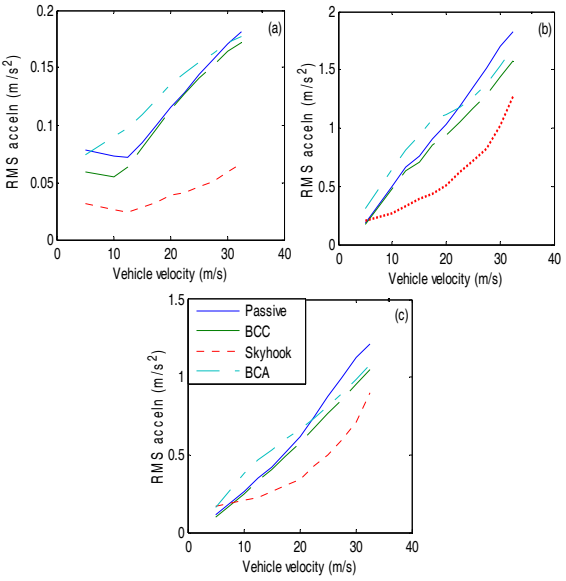

Fig. 3.13. RMS acceleration of the driver head-and-neck complex: (a) longitudinal direction, (b) vertical direction, (c) lateral direction [copyright IMechE (2008), reproduced from Tsampardoukas G, Stammers CW and Guglielmino E, Semi-active control of a passenger vehicle for improved ride and handling, accepted for publication in Proceedings of the Institution of Mechanical Engineers, Part D: Journal of Automobile Engineering, Publisher: Professional Engineering Publishing, ISSN 0954/4070, Vol 222, D3/2008, used by permission]